Mechanotransduction of fluid stresses governs 3D cell migration

William J. Polacheck[a], Alexandra E. German[b,c], Akiko Mammoto[c], Donald E. Ingber[c,d,e], and Roger D. Kamm[a,f,1]

[a]Department of Mechanical Engineering, Massachusetts Institute of Technology, Cambridge, MA 02139; [b]Harvard-MIT Division of Health Sciences and Technology, Cambridge, MA 02139; [c]Vascular Biology Program, Departments of Pathology and Surgery, Boston Children's Hospital and Harvard University Medical School, Boston, MA 02115; [d]Wyss Institute for Biologically Inspired Engineering, Harvard University, Boston, MA 02115; [e]Harvard School for Engineering and Applied Sciences, Cambridge, MA 02138; and [f]Department of Biological Engineering, Massachusetts Institute of Technology, Cambridge, MA 02139

Edited by Shu Chien, University of California, San Diego, La Jolla, CA, and approved January 6, 2014 (received for review September 7, 2013)

Solid tumors are characterized by high interstitial fluid pressure, which drives fluid efflux from the tumor core. Tumor-associated interstitial flow (IF) at a rate of ∼3 μm/s has been shown to induce cell migration in the upstream direction (rheotaxis). However, the molecular biophysical mechanism that underlies upstream cell polarization and rheotaxis remains unclear. We developed a microfluidic platform to investigate the effects of IF fluid stresses imparted on cells embedded within a collagen type I hydrogel, and we demonstrate that IF stresses result in a transcellular gradient in β1-integrin activation with vinculin, focal adhesion kinase (FAK), FAK^{PY397}, F actin, and paxillin-dependent protrusion formation localizing to the upstream side of the cell, where matrix adhesions are under maximum tension. This previously unknown mechanism is the result of a force balance between fluid drag on the cell and matrix adhesion tension and is therefore a fundamental, but previously unknown, stimulus for directing cell movement within porous extracellular matrix.

mechanobiology | breast cancer | metastasis

Integrins and associated focal adhesion (FA) proteins form a tension-sensitive mechanical link between the extracellular matrix (ECM) and the cytoskeleton, and serve as key components in the signaling cascade by which cells transduce mechanical signals into biological responses (mechanotransduction) (1, 2). Contractile stresses generated by the cell are balanced by tractions at cell–substrate adhesions, and the FA protein vinculin accumulates at regions of high substrate stress (3, 4). The FA protein paxillin colocalizes with vinculin (4) and mediates β1-integrin FA turnover through interaction with FA kinase (FAK) (5). The FAK–paxillin signaling axis recruits vinculin to β1 integrins at regions of high matrix adhesion tension (6), and paxillin—a key mechanosensor (7)—mediates protrusion formation at regions of high stress on 2D substrates (8), and FAK–paxillin–vinculin signaling is required for mechanosensing and durotaxis (9).

The tumor microenvironment imparts mechanical and chemical signals on tumor and stromal cells (10), and advanced breast carcinomas are characterized by high interstitial fluid pressure (11), an indicator of poor prognosis (12). This elevated fluid pressure drives interstitial flow (IF) and alters chemical transport within the tumor (13), and IF influences tumor cell migration through the generation of autocrine chemokine gradients (14). Equally important, although not as well understood, is the physical drag imparted on the ECM and constitutive cells (15) by IF, which is analogous to the FA-activating shear stresses generated on endothelial cells by hemodynamic forces (16). With endothelial cells, shear stress can be the dominant mechanical stimulus that induces FAK activation and cytoskeletal remodeling; however, for cells embedded within a porous matrix scaffold, the ratio of the force due to the pressure drop across the cell to the total shear force is inversely proportional to hydrogel permeability (*SI Appendix*, Eq. **S5**). In this study, we recapitulate physiologically relevant IF through collagen gel within a microfluidic device. Because the permeability of the collagen I hydrogel used in this study is small (1×10^{-13} m^2), the integrated pressure force is more than 30× the integrated shear force for a 20-μm-diameter cell (17) (*SI Appendix*, Eq. **S5**). To maintain static equilibrium, all fluid stresses imparted on the cell must be balanced by tension in matrix adhesions. In 2D, the adhesions balancing the fluid drag on the cell are confined to the basal cell surface, whereas in porous media, such as breast stromal ECM, matrix adhesions are distributed across the full cell surface. Consequently, maintaining static equilibrium requires greater adhesion tension on the upstream side of the cell to balance fluid stresses. From the reference frame of the cell, the effect of IF is mechanically equivalent to applying a net outward force at matrix adhesions on the upstream side of the cell, similar to the net tensile stresses applied by use of optical tweezers to study the molecular mechanisms underlying mechanotransduction (4, 18).

Here, we demonstrate that the forces required to balance drag imparted on the cell by IF induce a transcellular gradient in matrix adhesion tension, and the tensile stresses at the upstream side of the cell induce FA reorganization and polarization of FA-plaque proteins including vinculin, paxillin, FAK, FAK^{PY397}, and α-actinin. FA polarization leads to paxillin-dependent actin localization, the formation of protrusions upstream, and rheotaxis. Consistent with the governing mechanism of durotaxis on 2D substrates, this 3D mechanotransduction occurs through FAK and requires paxillin. Importantly, silencing paxillin does not affect cell migration speed but does attenuate rheotaxis. IF is present in many tissues in vivo (19), and because FA polarization and rheotaxis result from a mechanical force balance, this 3D mechanotransduction mechanism may be fundamental to all cells embedded within porous ECM.

Results

Microfluidic IF Platform. We developed a microfluidic platform consisting of two media channels separated by MDA-MB 231

Significance

Interstitial flow (IF) is elevated in solid tumors and imparts fluid stresses on tumor cells within the extracellular matrix (ECM), and these fluid stresses must be balanced by stress in matrix adhesions to maintain static equilibrium. This force balance results in greater matrix adhesion tension on the upstream side of the cell, and we demonstrate that this tension activates β1-integrin adhesion complexes, resulting in localization and activation of focal adhesion (FA) proteins near the upstream membrane. Importantly, we demonstrate that this asymmetric FA activation governs the direction of cell migration in 3D, and therefore our data show that mechanical stress acting on cells within a 3D ECM is a fundamental directional migratory stimulus.

Author contributions: W.J.P., A.E.G., A.M., and R.D.K. designed research; W.J.P. and A.E.G. performed research; A.E.G., A.M., and D.E.I. contributed new reagents/analytic tools; W.J.P., A.E.G., and R.D.K. analyzed data; and W.J.P., D.E.I., and R.D.K. wrote the paper.

The authors declare no conflict of interest.

This article is a PNAS Direct Submission.

[1]To whom correspondence should be addressed. E-mail: rdkamm@mit.edu.

This article contains supporting information online at www.pnas.org/lookup/suppl/doi:10.1073/pnas.1316848111/-/DCSupplemental.

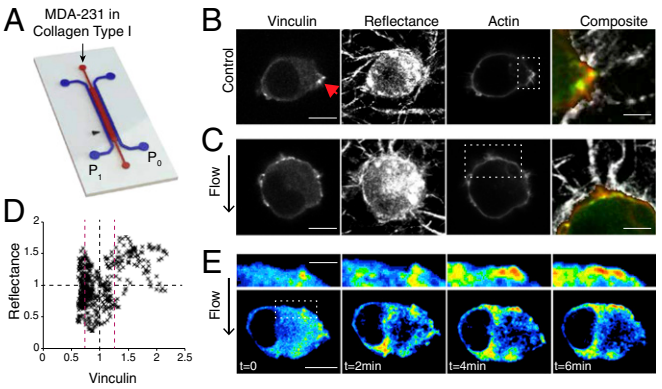

Fig. 1. IF induces reorganization of matrix adhesions. (*A*) Microfluidic platform for applying IF with collagen–cell suspension indicated in red and cell culture medium indicated in blue. The gel region is 200 μm deep, and a pressure gradient ($P_1 > P_0$) is established across the gel region to drive IF (red gel region is 2.3 mm in direction of flow). (*B*) MDA-MB 231 cells embedded within 2 mg/mL collagen gel are characterized by diffuse distribution of vinculin with regions of high vinculin concentration at the cell periphery (red arrow), where large collagen fibers are in contact with the cell, as seen in the reflectance channel (scale bar: 8 μm). Actin is confined to the periphery of the cell and colocalizes with vinculin. Composite images demonstrate that regions of intense vinculin and actin staining correspond to regions where collagen fibers extend radially outward from the cell surface (red = actin, green = vinculin, and gray = reflectance) (scale bar: 3 μm). (*C*) A flow of 4.6 μm/s for 4 h induces vinculin and actin localization at the upstream edge of the cell (scale bar: 9 μm). Composite images demonstrate upstream localization of actin and vinculin where the cell is in contact with collagen (red = actin, green = vinculin, and gray = reflectance) (scale bar: 3 μm). (*D*) Colocalization of vinculin and collagen at the cell membrane, where each data point represents a location on the cell membrane. Regions where vinculin intensity is greater than the mean (vertical black dashed line) ± SD (red dashed lines) correspond to regions with high reflectance intensity. (*E*) Vinculin accumulates rapidly at the upstream side of the cell. The 16-color intensity heatmaps (red = max and blue = min) demonstrate intense vinculin localization within 4 min of initiating 4.6 μm/s flow [scale bar *Lower*: 8 μm; *Upper* (*Insets*): 3 μm].

mammary adenocarcinoma cells embedded in a collagen type I hydrogel (Fig. 1*A*) (17, 20). By holding one medium channel (upstream) at a higher fluid pressure than the other channel (downstream), a stable and repeatable flow field can be generated through the collagen gel (Movie S1 and *SI Appendix*, Fig. S2). We introduced a 60-Pa pressure gradient across the 2 mg/mL collagen gel to drive flow with a mean velocity of 4.6 μm/s, as measured along the center line of the device. The total fluid drag force imparted on a spherical cell can be estimated from the solution for drag on a sphere within a Brinkman medium (21), and for our experimental setup, a 16.8 pN integrated shear force and 235 pN integrated pressure force are imparted on a 20-μm-diameter cell (*SI Appendix*, Eq. **S5**). The fluid drag imparted on the cell is balanced by tension generated in matrix adhesions, and by imaging a cell as flow is applied it can be seen that flow induces tension in upstream matrix adhesions, which are well connected to the cell surface (Movie S2 and *SI Appendix*, Fig. S3).

MDA-MB 231 cells embedded within 2 mg/mL 3D collagen type I gels displayed diffuse distribution of vinculin and less prominent punctate vinculin aggregates than when cultured on 2D glass substrates coated with collagen type I. F actin was localized to the cell periphery rather than traversing the cells in stress fibers as in 2D (Fig. 1*B* and *SI Appendix*, Fig. S4), and actin colocalized with vinculin (*SI Appendix*, Fig. S4*F*). When cells were exposed to 4.6 μm/s flow for 4 h, vinculin and actin localized at the upstream edge of the cell, whereas the density of collagen as measured by confocal reflectance microscopy was reduced at the downstream edge of the cell (Fig. 1*C*). The vinculin asymmetry induced by flow is due to an increase in FA-like vinculin clusters on the upstream side of the cell (*SI Appendix*, Fig. S4*G*), and these FA-like clusters occur at regions where collagen is bound to the cell surface (Fig. 1*D*). Vinculin accumulation at regions of stress occurs rapidly (22), as vinculin localized to the upstream portion of the cell within 4 min of applying flow (Fig. 1*E*). Although NIH 3T3 fibroblasts and MCF10A breast epithelial cells did not demonstrate the more punctate, FA-like vinculin-containing adhesions characteristic of the MDA-MB 231 cells, exposure to 4.6 μm/s flow for 4 h increased vinculin and actin accumulation at the upstream side of the cell for both the NIH 3T3 fibroblasts and MCF10A breast epithelial cells (*SI Appendix*, Fig. S5).

IF Induces FA Reorganization and Upstream Polarization of FA Proteins. Integrin-based mechanotransduction involves a cohort of FA plaque proteins that accumulate at regions of locally applied stress and localize with vinculin and actin. In particular, adhesions containing paxillin elongate under applied traction (23). FAK also becomes autophosphorylated at Tyr 397 through binding with β1 integrins in endothelial cells in response to shear stress (24) and in breast adenocarcinoma cells when exposed to 3 μm/s IF as we have shown previously (17). Furthermore, phosphorylation of FAK at Tyr 397 is required for invadopodia formation for breast cancer cells (25), and FAK^{PY397} is differentially expressed in metastatic cervical carcinoma relative to noncancerous epithelium (26). FAK is required for mechanical stress-induced cell polarization (6, 27), and the FAK–paxillin–vinculin signaling complex is required for rigidity sensing and durotaxis (9). To quantify the localization of FA proteins, we defined a normalized metric to measure the distribution of fluorescently tagged proteins at the cell membrane. A polarization metric is computed by measuring the average intensity at the upstream and downstream edges of the cell (I_{Up} and I_{Down}, respectively) for the median slice of a confocal image stack acquired for each cell (Eq. **1** and Fig. 2):

$$Polarization = \frac{\langle I_{Up}\rangle - \langle I_{Down}\rangle}{(\langle I_{Up}\rangle + \langle I_{Down}\rangle)/2}. \quad [1]$$

IF (4.6 μm/s flow for 4 h) caused a statistically significant increase in polarization for vinculin, actin, and collagen (Fig. 2);

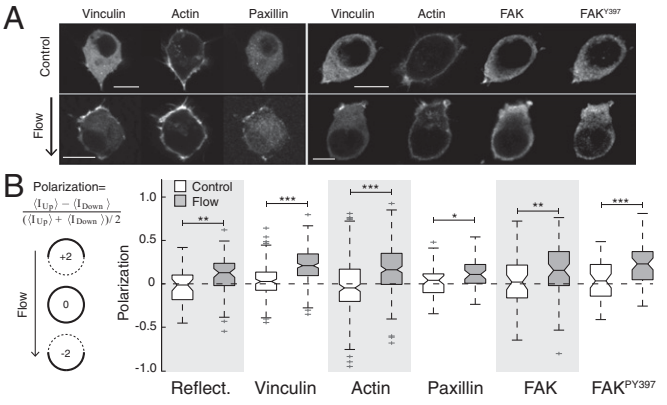

Fig. 2. Focal adhesion proteins localize to the upstream side of cells exposed to IF. (*A*) In control devices, paxillin, FAK, and FAK^{PY397} are distributed diffusely throughout the cell cytoplasm but weakly colocalize with actin and vinculin at the cell periphery. Flow induces upstream polarization of each protein. (Scale bars: 10 μm.) (*B*) Polarization is measured by the relative upstream fluorescence intensity of each signal at the cell membrane; +2 is the maximum upstream polarization, whereas −2 is the maximum downstream polarization. Upstream polarization increases for collagen ECM, vinculin, actin, paxillin, FAK, and FAK^{PY397} in cells exposed to 4.6 μm/s flow for 4 h. For each box, center mark is the median; notches encompass 95% confidence interval of the median; lower and upper box edges are 25th and 75th percentiles; whiskers are data range; and + symbols are outliers. (***$P < 0.001$, **$P < 0.01$, and *$P < 0.05$ calculated from Wilcoxon rank-sum test with >45 cells from more than three devices for each condition).

in all cases cells' higher polarization for vinculin correlated with higher polarization for actin (*SI Appendix*, Fig. S4*H*). The fraction of the cell population with upstream polarization increased with flow; 81% of cells exposed to 4 h of flow displayed polarization values greater than control (no flow), and 50.2% displayed values greater than the mean + 1 SD (compared with 48% and 14%, respectively for control). A similar trend was observed for actin, with polarization of 77% of cells with flow greater than controls and 33% of cells exposed to flow greater than the mean + 1 SD (compared with 47.7% and 14%, respectively for control).

Furthermore, flow increased polarization of paxillin, FAK, and FAK^{PY397}, indicating that these FA plaque proteins localize to the upstream cell periphery under flow (Fig. 2). IF also induced upstream localization of α-actinin (*SI Appendix*, Fig. S5*C*), an actin–cross-linking protein critical for the extension of lamellipodia in 2D (28) that localizes to regions of traction applied by magnetic tweezer (29).

FA Protein Polarization Occurs via β1-Integrin Signaling. Blocking β1-integrin ligation by treating cells with anti-beta1-integrin-blocking antibodies (30) attenuated the polarization of actin and vinculin in response to flow. The cells remained nearly spherical, and vinculin and actin were distributed evenly around the cell perimeter even when exposed to IF (Fig. 3 *A* and *B*), providing evidence that β1-integrin ligation and signaling are required for actin and vinculin polarization in response to flow. The collagen matrix becomes anisotropically distributed under flow (Fig. 2*B*), and we hypothesize that FA plaque protein polarization is a consequence of the dense matrix on the upstream side of the cell, which presents more adhesion sites than the downstream matrix. When cells were incubated with aprotinin, a broad matrix metalloproteinase (MMP) inhibitor that mediates ECM remodeling (31), the pericellular matrix remained isotropically distributed under flow, but vinculin and actin still localized upstream, indicating that FA polarization is not due to the observed IF-induced changes in ECM density (Fig. 3 *C* and *D*). Shi et al. found a heparan sulfate proteoglycan (HSPG)-mediated increase in smooth muscle cell motility in response to IF (32). We therefore incubated cells with heparinase to degrade the cell-associated HSPG and applied flow for 4 h. We found that actin and vinculin polarization persisted, suggesting that the cell polarization observed in our experiments in response to IF is not mediated by HSPG (Fig. 3*E*).

Miyamoto et al. determined that tyrosine kinase activity is required for the formation of mature FAs and for the accumulation of most FA plaque proteins, including F actin, paxillin, and FAK, to nascent FAs (2). However, the authors found that vinculin still localized to β1-integrins in response to integrin ligation even when cells were treated with genistein, a broad tyrosine kinase inhibitor. In our experiments, genistein attenuated the upstream accumulation of actin, FAK, and FAK^{PY397} in response to flow such that no statistical difference was observed in polarization between the static and flow cases. However, polarization for vinculin increased with flow and 69% of cells demonstrated a polarization value greater than the mean for the static samples (Fig. 3 *F* and *G*), demonstrating that vinculin polarization is maintained even in the absence of tyrosine kinase activity, but tyrosine kinase activity is required for recruitment of FAK, FAK^{PY397}, and actin.

Paxillin Is Required for Upstream Actin Polarization and Protrusion Formation. Paxillin is required for stiffness mechanosensing (6), protrusion formation at regions of high stress (8), and durotaxis (9). To evaluate the role of paxillin in upstream FA polarization and rheotaxis, we treated cells with paxillin siRNA, resulting in knockdown of paxillin expression by 80% as confirmed by immunoblotting (Fig. 4*A*) and quantitative RT-PCR (*SI Appendix*, Fig. S6), and no change in vinculin expression was observed (Fig. 4*A*). Paxillin siRNA induced an irregular cell morphology with increased protrusions and decreased polarization of vinculin and actin under flow (Fig. 4*B*). Flow-induced polarization of vinculin was attenuated with paxillin siRNA (Fig. 4*C*), whereas paxillin siRNA blocked actin polarization (Fig. 4*D*), a similar trend to the effect of blocking tyrosine phosphorylation.

Actin polymerization and protrusion formation are required for cell migration in 3D ECMs, and the number of protrusions per cell in 2D scales with motility of MDA-MB 231 cells in 3D (33). Exposing cells to 4.6 μm/s flow for 4 h caused a decrease in protrusion formation, but cells extended more protrusions in the upstream direction (Fig. 4 *E* and *F*). Mean circularity (the ratio of the square of the cell perimeter to the cell area, circularity = 1 for a circle) decreased with flow (Fig. 4*E*). To determine the relative number of protrusions upstream and downstream, we divided maximum intensity projections of an actin stain into thirds by area and compared the upstream perimeter to the downstream perimeter (Fig. 4*F*). With flow, the relative upstream perimeter increased (Fig. 4*G*) due to the extension of protrusions upstream (Movie S3 and *SI Appendix*, Fig. S7), and these actin-rich upstream protrusions colocalized with cortactin (*SI Appendix*, Fig. S7*D*), a marker for cell polarity and the leading edge for cell migration in 3D (34). For both control and flow conditions, paxillin siRNA significantly increased the number of protrusions, as

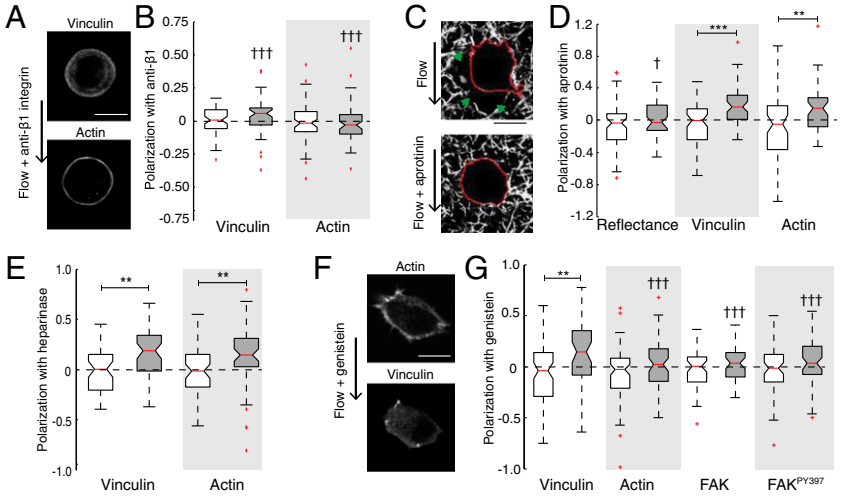

Fig. 3. FA reorganization is mediated by β1 integrins. (*A*) Cells treated with anti–β1-integrin–blocking antibodies displayed a spherical morphology with actin and vinculin isotropically distributed at the cell periphery. (*B*) Anti–β1-integrin–blocking antibodies attenuate actin and vinculin localization at the upstream cell edge, and there is no statistically significant difference in polarization of actin and vinculin with and without flow (white, control; gray, flow, for all graphs). (*C*) The MMP inhibitor, aprotinin, blocks flow-induced ECM remodeling (downstream gaps in the matrix indicated by green arrows), resulting in isotropically distributed pericellular matrix. (*D*) MMP inhibition by treatment with aprotinin attenuates polarization of ECM with flow, but vinculin and actin remain polarized and localize upstream. (*E*) Flow causes vinculin and actin polarization in cells treated with heparinase, which degrades HPSGs, demonstrating that the upstream FA and cytoskeletal polarization occur independent of the glycocalyx. (*F*) Genistein, a broad tyrosine kinase inhibitor, reduced polarization of actin, FAK, and FAK^{PY397}. (*G*) Inhibition of tyrosine kinase activity with genistein attenuated the polarizing effects of flow on actin, FAK, and FAK^{PY397}, although polarization of vinculin persisted. (Scale bars: 10 μm.) More than 45 cells from more than three devices for each condition. $^{***}P < 0.001$, $^{**}P < 0.01$, and $^{*}P < 0.05$ calculated from Wilcoxon rank-sum test. $^{\dagger}P < 0.05$ and $^{\dagger\dagger\dagger}P < 0.001$ measured vs. equivalent flow case with no drug applied. For each box, red center line is the median; notches encompass 95% confidence interval of the median; lower and upper box edges are 25th and 75th percentiles; whiskers are data range; and red + symbols are outliers.

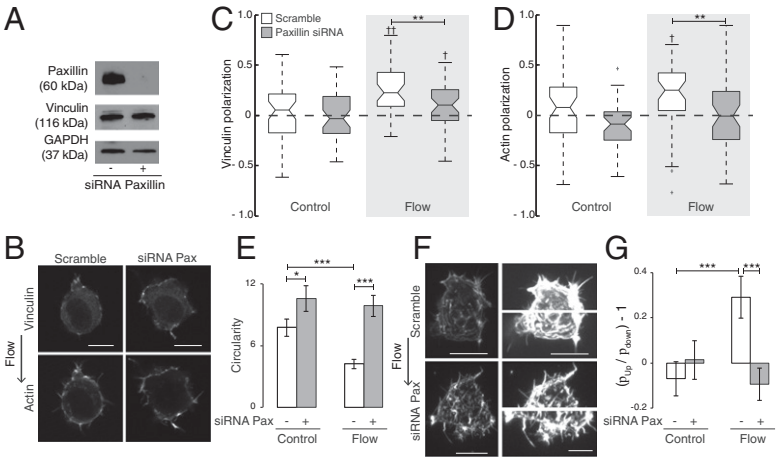

Fig. 4. IF induces paxillin-dependent protrusion formation at the upstream cell membrane. (*A*) Immunoblots showing paxillin, vinculin, and GAPDH protein levels in MDA-MB 231 cells transfected with scramble control or paxillin-targeted siRNA. (*B*) Cells treated with paxillin siRNA demonstrate isotropically distributed actin, and vinculin-containing adhesions localize both upstream and downstream. (*C* and *D*) Paxillin siRNA attenuates polarization of vinculin (*C*) and completely blocks polarization of actin (*D*). (*E*) Paxillin siRNA increases the number of protrusions for both control and flow as measured by circularity, a nondimensional measure of the square of cell perimeter normalized by cell area (1 for a circle). (*F*) Maximum actin intensity projections of a cell exposed to flow for 4 h. Actin is more densely localized at the upstream membrane than on the downstream. (Scale bar *Left*: 10 μm.) Magnified images of the upstream and downstream 1/third of the cell as measured by area demonstrate more protrusions at the upstream cell membrane for cells exposed to flow. (Scale bar *Right*: 5 μm.) Cells treated with paxillin siRNA demonstrate more protrusions with no directional bias. (*G*) The difference in perimeter between the upstream and downstream one-third of each cell area (as depicted in *F*) demonstrates that under flow, more protrusions form in the upstream direction, and paxillin siRNA attenuates the upstream protrusion bias. For each box, center mark is the median; notches encompass 95% confidence interval of the median; lower and upper box edges are 25th and 75th percentiles; whiskers are data range; and + symbols are outliers. More than 45 cells from more than three devices for each condition, $***P < 0.001$, $**P < 0.01$, and $*P < 0.05$, calculated from Wilcoxon rank-sum test. $^{\dagger}P < 0.05$ and $^{\dagger\dagger}P < 0.01$ measured vs. no-flow control.

indicated by the higher values of circularity under control conditions (Fig. 4*E*), and interestingly, there was no observable upstream protrusion bias for cells treated with paxillin siRNA (Fig. 4*G*).

IF Induces Paxillin-Dependent Rheotaxis. IF has been shown to induce rheotaxis when cells are seeded at sufficiently high density for paracrine chemokine fields to interfere with autocrine chemokine fields (17), and cells migrating upstream have been shown to migrate with increased persistence (35). We seeded cells at a density shown to induce preferential upstream migration of MDA-MB 231 (6×10^5 cells per mL) and applied 4.6 μm/s flow for 8 h, tracking the cells by taking images every 15 min. Cells preferentially migrated upstream (Fig. 5*A*) with increased directionality (net migration distance normalized by total migration distance; *SI Appendix*, Fig. S8) although migration speed was unaffected by flow (*SI Appendix*, Fig. S8). Paxillin knockdown attenuated upstream migration (Fig. 5*B*) and reduced flow-induced increases in directionality (*SI Appendix*, Fig. S8), but migration speed was unaffected (*SI Appendix*, Fig. S8), consistent with the results using a scratch assay in fibroblasts (8).

To further evaluate the effect of flow on the direction of cell migration, the direction of the net migration vectors for each cell in four separate devices (>300 tracks per condition) were plotted in polar histograms (Fig. 5*C*). Flow induced a dramatic increase in the fraction of cells migrating upstream, whereas treatment of cells with paxillin siRNA reversed the directional bias, causing more cells to migrate downstream than upstream (Fig. 5*C*). The difference between the fraction of cells migrating upstream and the fraction migrating downstream was calculated for each device, and flow caused a significant increase in the relative fraction of cells migrating upstream (Fig. 5*D*). Paxillin was required for the upstream migration bias, with paxillin knockdown causing a significant decrease in the relative fraction migrating upstream with flow, and in fact, a net downstream migration bias is observed with flow and paxillin siRNA (Fig. 5*D*).

Discussion

These studies show that interstitial fluid flow induces a transcellular gradient in matrix adhesion stress inducing adhesion activation, cell polarization, and migration toward regions of maximum adhesion tension (Fig. 6). This response is mediated by tension-sensitive β1-integrin complexes and results from a force balance required to maintain static equilibrium. Integrins are under maximum tension at the upstream side of the cell (Fig. 6), and tension-induced FA-associated protein localization upstream leads to actin accumulation and membrane protrusion in the upstream direction, eventually leading to upstream migration. The trends for directional protrusion extension are strikingly similar to the trends for the direction of cell migration (Figs. 4*G* and 5*D*), consistent with the observation that protrusion formation is a marker for 3D motility of MDA-MB-231 cells (33).

Here, we provide evidence for a paxillin-dependent mechanism by which FA activation leads to protrusion formation and migration in porous scaffolds (Fig. 6). Actin localization upstream requires paxillin and tyrosine kinase activity; vinculin, on the other hand, remains localized upstream, but the extent of polarization decreases when tyrosine phosphorylation is inhibited

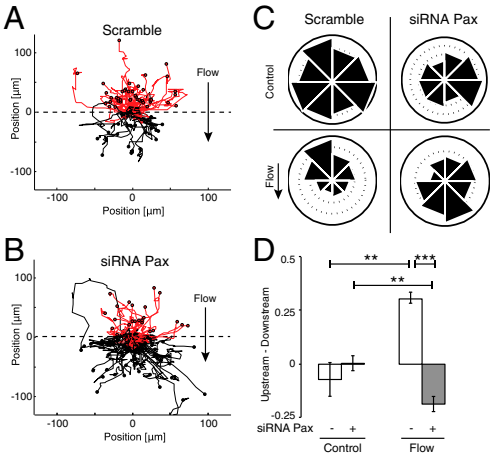

Fig. 5. IF induces paxillin-dependent rheotaxis. (*A*) Sample migration tracks demonstrate upstream migration over 8 h when exposed to flow. Migration tracks with a net upstream displacement are colored red and downstream tracks are black (for clarity, only tracks from cells that migrated >30 μm over 8 h are shown). (*B*) Treatment with paxillin siRNA reduces upstream migration. (*C*) Polar histograms of the direction of net displacement for each cell tracked over 8 h (>300 tracks from four devices per condition) demonstrate flow-induced rheotaxis, which is attenuated with paxillin siRNA. (*D*) Difference between the fraction of cells migrating upstream and downstream for each condition in *C* (error bars are standard error of the mean; $**P < 0.01$ and $***P < 0.001$ calculated by one-way ANOVA).

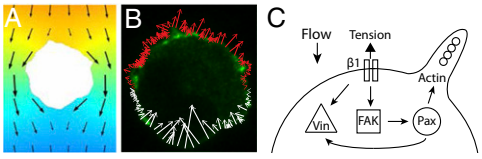

D

Condition	Vinculin Localization	Actin Localization	Migration	Dir. Migration
Control	-	-	+	-
Flow	++	+	+	+
Flow+siPax	+	-	+	-
Flow+genistein	+	-	-	-
Flow+anti-beta1	-	-	-	-

Fig. 6. Mechanotransduction induces rheotaxis. (*A*) Simulation of flow past the cell in Fig. 1*C*, with inlet velocity of 4.6 μm/s, local fluid velocity vectors in black superimposed on a heat map of pressure (orange = maximum and blue = minimum). (*B*) Local reaction forces (red arrows = tensile and white arrows = compressive) in cell-matrix connections required to maintain static equilibrium when exposed to flow profile in A) superimposed on an image of vinculin distribution. Vinculin localizes to regions of cell-matrix tension. (*C*) Integrin activation by local flow-induced tension induces vinculin, FAK, paxillin, and actin localization, and subsequent protrusion extension at the upstream cell membrane. (*D*) Table showing upstream localization of vinculin is maintained in the absence of paxillin or when tyrosine kinase activity is blocked, but actin localization and subsequent protrusion extension, and upstream migration require both tyrosine kinase activity and functional paxillin.

and when paxillin is silenced. These data are consistent with the observations of Pasapera et al., who demonstrated that vinculin is recruited to FAs by two separate pathways (6) (Fig. 6). In one pathway, tension across β1 integrins is transmitted to talin, opening cryptic binding domains in talin and allowing vinculin to bind independent of kinase activity (2, 36, 37). The second pathway involves tension-mediated FAK phosphorylation at Tyr 397. This allows for the formation of the FAK-Src signaling complex and phosphorylation of paxillin at Tyr 31 and Tyr 118, which recruits vinculin and causes FA maturation (6). Consequently, the integrin–talin–vinculin pathway can be activated even in the absence of paxillin or tyrosine kinase activity, but full FA maturation, culminating in protrusion extension and migration, requires paxillin and tyrosine kinase activity.

In addition to imparting fluid stresses, IF convects autocrine factors downstream, causing gradients of autologously secreted chemokines that have been shown to direct migration downstream in response to IF (14). Furthermore, we have shown previously that at high cell densities, autocrine chemokine fields overlap with fields from neighboring cells, reducing transcellular autocrine gradients and inducing preferential upstream migration (17). In this study, cells were seeded at a sufficiently high density (6×10^5 cells per mL) and flow rate to minimize contributions from autocrine gradients, leading to upstream migration. Silencing paxillin, however, caused cells to preferentially migrate downstream (Fig. 5*C*), consistent with the hypothesis that IF induces simultaneous competing upstream and downstream stimuli.

In the present experiments, 4.6 μm/s IF imparts ∼1 Pa (1 pN/μm^2) average stress to the cell due to the pressure drop across the cell length, and the integrated force due to the pressure drop is greater than 30× the integrated shear force (*SI Appendix*, Eq. **S5**). This stress profile is distinctly different from that in cells exposed to shear stress in 2D, where shear stress is the dominant component to the fluid drag imparted on the cell (24). Images of the collagen matrix obtained from confocal reflectance imaging, however, demonstrate that only a fraction of the cell surface is adhered to the local matrix (Fig. 1*C*). Estimating that 20% of the cell area adhered to matrix fibers (fraction of reflectance pixels at cell boundary greater than mean + SD reflectance intensity in Fig. 1*C*), stress at matrix adhesions is amplified to 5 pN/μm^2 stress. This level of stress falls within the range of stresses that have been shown to activate FAs on 2D surfaces (3–12 pN/μm^2 induces local actin recruitment in regions of applied stress via optical tweezer) (18). The same levels of stress asymmetry could be generated with much lower flow rates in vivo due to the 3 orders of magnitude lower permeability (*SI Appendix*, Eq. **S6**) (38), suggesting that even nonpathologic IF velocities (<1 μm/s) would result in an asymmetry in matrix adhesion tension and promote directional migration.

Importantly, we also demonstrate that paxillin is required for directional protrusion formation and rheotaxis, which is consistent with the observation that paxillin is required for protrusion formation toward regions of maximum adhesion tension on 2D substrates (39). It is also known that phosphorylated paxillin enhances lamellipodial activity for cells on 2D substrates (5), and importantly, the FAK–paxillin–vinculin signaling axis is instrumental in durotaxis (9). Consequently, the mechanism and relevant signaling pathways responsible for rheotaxis in 3D ECM may be similar to the mechanism underlying durotaxis for cells on 2D substrates, where cells migrate in response to gradients in matrix adhesion tension that result from myosin-dependent cell contraction on substrates with a gradient in mechanical stiffness (40). Cells exert greater force against a stiff substrate than a soft one (40), so the normal stresses are higher against a stiff ECM, causing migration in the direction of the stiffer matrix. The mechanism has been further tested by applying force to the cell directly, and FAs are activated and recruit vinculin at regions of high substrate adhesion stress (23). Therefore, the mechanism underlying rheotaxis and durotaxis may be the same, where stress asymmetry at matrix adhesions induces migration toward adhesions under maximum tension, and here we demonstrate that this mechanism, which has been demonstrated for cells cultured on a 2D substrate (23, 40), directs cell processes and migration in physiologically relevant 3D microenvironments.

Although these experiments were conducted on a single cell type, we expect mechanotransduction of IF stresses to be a generally relevant mechanism that influences the morphology and function of cells expressing β1 integrins embedded within tissues experiencing IF (19), and we have found that flow induces polarization of vinculin for MCF10A breast epithelial cells and NIH 3T3 fibroblasts (*SI Appendix*, Fig. S5). For example, cells in the vicinity of an artery, vein, or lymphatic vessel are exposed to IF, and the present data suggest that the stresses imparted on these cells would influence cell morphology and migration. Indeed, basal-to-apical transendothelial flow has been shown to induce vascular sprouting angiogenesis via tension between the ECM and basal adhesions, but not when the adhesions are compressed by apical-to-basal flow (41). In these experiments, the basal cell surface adheres to collagen via β1 integrins, and basal-to-apical flow generates tension in the basal β1 integrins, in much the same way that flow generates tension at upstream matrix adhesions in the present experiments. Furthermore, basal-to-apical flow induced phosphorylation of FAK at Y397 and localization of actin to the basal cell surface, consistent with the effect of IF on tumor cells, and sprouting was inhibited by genistein, which inhibited cell migration in the present experiments (*SI Appendix*, Fig. S8*C*).

Cells experience asymmetric stresses in vivo under various conditions. For example, cell contraction induces deformation of the local matrix, and this deformation is propagated through the ECM to neighboring cells (42). For endothelial cells on 2D surfaces, traction generated by one cell can be transmitted to a neighboring cell inducing protrusion formation and migration toward the contractile cell (43). These data are consistent with our observations in 3D that local tension drives protrusion extension and migration and suggest that stress asymmetries play a role in a variety of cell processes in vivo. Because paxillin appears to mediate cellular responses to IF, and it is also known to be involved in tumor progression and metastasis in many types of cancer (44), modulation of paxillin levels or activity could offer a therapeutic strategy for treating metastatic carcinoma. Importantly, in solid tumors, interstitial fluid flow emanates from the vasculature, and consequently, tumor cells in close proximity to blood vessels will be directed via rheotaxis toward the leaky vasculature, which is the point of maximum fluid pressure (45). Therefore, lowering IF velocity magnitude (by reducing interstitial

fluid pressure) (46) could reduce tumor cell migration toward vasculature in vivo and render metastatic disease more treatable.

Materials and Methods

Cell Seeding. Microfluidic devices were fabricated via soft lithography as described previously (47). MDA-MB 231 cells derived from pleural effusion were purchased from the American Type Culture Collection and cultured in growth medium comprised of DMEM (Invitrogen) with 10% (vol/vol) FBS (Invitrogen). Collagen type I in acetic acid (BD Biosciences) was buffered with 10× PBS, titrated to a pH of 8.9 with 0.1 M sodium hydroxide, and brought to a final concentration of 2 mg/mL with water. Cells were harvested with Trypsin/EDTA and centrifuged at 200 × *g* for 5 min. Cells were resuspended in growth medium and mixed with collagen I solution for a final concentration of 6×10^5 cells per mL total collagen solution. Collagen was polymerized in humidified chambers at 37 °C and 5% CO_2 for 20 min, and after gelation, growth medium was added to hydrate the gel. Integrin and MMP blocking and heparinase treatment are described in detail in *SI Appendix*.

Transfection and Selection. MDA-MB 231 cells stably expressing vinculin–GFP fusion protein were generated by lipid transfection and neomyocin selection (*SI Appendix, Supplementary Methods*). The vinculin–GFP plasmid has been described and characterized previously (48) and was a gracious gift of Benjamin Geiger (Weizmann Institute of Science, Rehovot, Israel). siRNA against human paxillin (GTGTGGAGCCTTCTTTGGT) was purchased from Sigma Genosys (8). Cells were transfected with SiLentFect according to the manufacturer's protocol (Bio-Rad) (*SI Appendix, Supplementary Methods*).

Applying IF. After gelation of the collagen gel, cells were incubated for 12–24 h at 37 °C and 5% CO_2 before applying flow. To apply a pressure gradient, external media reservoirs were connected to the microfluidic chip, and growth medium, anti–b1-integrin blocking medium or heparinase- or aprotinin-containing medium was added to the reservoir to establish a pressure gradient across the collagen gel (60 Pa pressure drop for 4.6 μm/s flow). For migration experiments, culture medium was supplemented with 20 ng/mL human epidermal growth factor (PeproTech) to stimulate cell migration (17). Phase contrast images were taken every 15 min for 8 h in an environmental chamber held at 37 °C and 5% CO_2. Fixation, staining, and imaging are described in detail in *SI Appendix*.

ACKNOWLEDGMENTS. We thank Hyundo Lee and Hyung Wan Do for assistance with figure design and Simon Gordonov and Dr. Shannon Hughes for assistance in imaging actin dynamics. Funding from National Cancer Institute R21CA140096 and R33CA174550, the Singapore–Massachusetts Institute of Technology Alliance for Research and Technology, and Department of Defense Breast Cancer Innovator Award BC074986 (to D.E.I.) is greatly appreciated. W.J.P. and A.E.G. are supported by National Science Foundation Graduate Research Fellowships.

1. Moore SW, Roca-Cusachs P, Sheetz MP (2010) Stretchy proteins on stretchy substrates: The important elements of integrin-mediated rigidity sensing. *Dev Cell* 19(2):194–206.
2. Miyamoto S, et al. (1995) Integrin function: Molecular hierarchies of cytoskeletal and signaling molecules. *J Cell Biol* 131(3):791–805.
3. Balaban NQ, et al. (2001) Force and focal adhesion assembly: A close relationship studied using elastic micropatterned substrates. *Nat Cell Biol* 3(5):466–472.
4. Galbraith CG, Yamada KM, Sheetz MP (2002) The relationship between force and focal complex development. *J Cell Biol* 159(4):695–705.
5. Zaidel-Bar R, Milo R, Kam Z, Geiger B (2007) A paxillin tyrosine phosphorylation switch regulates the assembly and form of cell-matrix adhesions. *J Cell Sci* 120(Pt 1):137–148.
6. Pasapera AM, Schneider IC, Rericha E, Schlaepfer DD, Waterman CM (2010) Myosin II activity regulates vinculin recruitment to focal adhesions through FAK-mediated paxillin phosphorylation. *J Cell Biol* 188(6):877–890.
7. Sero JE, German AE, Mammoto A, Ingber DE (2012) Paxillin controls directional cell motility in response to physical cues. *Cell Adhes Migr* 6(6):502–508.
8. Sero JE, et al. (2011) Paxillin mediates sensing of physical cues and regulates directional cell motility by controlling lamellipodia positioning. *PLoS ONE* 6(12):e28303.
9. Plotnikov SV, Pasapera AM, Sabass B, Waterman CM (2012) Force fluctuations within focal adhesions mediate ECM-rigidity sensing to guide directed cell migration. *Cell* 151(7):1513–1527.
10. Polacheck WJ, Zervantonakis IK, Kamm RD (2013) Tumor cell migration in complex microenvironments. *Cell Mol Life Sci* 70(8):1335–1356.
11. Stylianopoulos T, et al. (2013) Coevolution of solid stress and interstitial fluid pressure in tumors during progression: Implications for vascular collapse. *Cancer Res* 73(13):3833–3841.
12. Milosevic M, et al. (2001) Interstitial fluid pressure predicts survival in patients with cervix cancer independent of clinical prognostic factors and tumor oxygen measurements. *Cancer Res* 61(17):6400–6405.
13. Chauhan VP, Stylianopoulos T, Boucher Y, Jain RK (2011) Delivery of molecular and nanoscale medicine to tumors: Transport barriers and strategies. *Annu Rev Chem Biomol Eng* 2:281–298.
14. Shields JD, et al. (2007) Autologous chemotaxis as a mechanism of tumor cell homing to lymphatics via interstitial flow and autocrine CCR7 signaling. *Cancer Cell* 11(6):526–538.
15. Pedersen JA, Lichter S, Swartz MA (2010) Cells in 3D matrices under interstitial flow: Effects of extracellular matrix alignment on cell shear stress and drag forces. *J Biomech* 43(5):900–905.
16. Tarbell JM, Weinbaum S, Kamm RD (2005) Cellular fluid mechanics and mechanotransduction. *Ann Biomed Eng* 33(12):1719–1723.
17. Polacheck WJ, Charest JL, Kamm RD (2011) Interstitial flow influences direction of tumor cell migration through competing mechanisms. *Proc Natl Acad Sci USA* 108(27):11115–11120.
18. Icard-Arcizet D, Cardoso O, Richert A, Hénon S (2008) Cell stiffening in response to external stress is correlated to actin recruitment. *Biophys J* 94(7):2906–2913.
19. Rutkowski JM, Swartz MA (2007) A driving force for change: Interstitial flow as a morphoregulator. *Trends Cell Biol* 17(1):44–50.
20. Farahat WA, et al. (2012) Ensemble analysis of angiogenic growth in three-dimensional microfluidic cell cultures. *PLoS ONE* 7(5):e37333.
21. Ganapathy R (1997) Creeping flow past a solid sphere in a porous medium. *Z Angew Math Mech* 77:871–875.
22. Allioux-Guérin M, et al. (2009) Spatiotemporal analysis of cell response to a rigidity gradient: A quantitative study using multiple optical tweezers. *Biophys J* 96(1):238–247.
23. Riveline D, et al. (2001) Focal contacts as mechanosensors: Externally applied local mechanical force induces growth of focal contacts by an mDia1-dependent and ROCK-independent mechanism. *J Cell Biol* 153(6):1175–1186.
24. Li S, et al. (1997) Fluid shear stress activation of focal adhesion kinase. Linking to mitogen-activated protein kinases. *J Biol Chem* 272(48):30455–30462.
25. Chan KT, Cortesio CL, Huttenlocher A (2009) FAK alters invadopodia and focal adhesion composition and dynamics to regulate breast cancer invasion. *J Cell Biol* 185(2):357–370.
26. Grisaru-Granovsky S, et al. (2005) Differential expression of protease activated receptor 1 (Par1) and pY397FAK in benign and malignant human ovarian tissue samples. *Int J Cancer* 113(3):372–378.
27. Wang HB, Dembo M, Hanks SK, Wang YL (2001) Focal adhesion kinase is involved in mechanosensing during fibroblast migration. *Proc Natl Acad Sci USA* 98(20):11295–11300.
28. Choi CK, et al. (2008) Actin and alpha-actinin orchestrate the assembly and maturation of nascent adhesions in a myosin II motor-independent manner. *Nat Cell Biol* 10(9):1039–1050.
29. Wang N, Butler JP, Ingber DE (1993) Mechanotransduction across the cell surface and through the cytoskeleton. *Science* 260(5111):1124–1127.
30. Ahmed N, Riley C, Rice G, Quinn M (2005) Role of integrin receptors for fibronectin, collagen and laminin in the regulation of ovarian carcinoma functions in response to a matrix microenvironment. *Clin Exp Metastasis* 22(5):391–402.
31. Yeon JH, Ryu HR, Chung M, Hu QP, Jeon NL (2012) In vitro formation and characterization of a perfusable three-dimensional tubular capillary network in microfluidic devices. *Lab Chip* 12(16):2815–2822.
32. Shi Z-D, Wang H, Tarbell JM (2011) Heparan sulfate proteoglycans mediate interstitial flow mechanotransduction regulating MMP-13 expression and cell motility via FAK-ERK in 3D collagen. *PLoS ONE* 6(1):e15956.
33. Meyer AS, et al. (2012) 2D protrusion but not motility predicts growth factor-induced cancer cell migration in 3D collagen. *J Cell Biol* 197(6):721–729.
34. Petrie RJ, Gavara N, Chadwick RS, Yamada KM (2012) Nonpolarized signaling reveals two distinct modes of 3D cell migration. *J Cell Biol* 197(3):439–455.
35. Haessler U, Teo JCM, Foretay D, Renaud P, Swartz MA (2012) Migration dynamics of breast cancer cells in a tunable 3D interstitial flow chamber. *Integr Biol (Camb)* 4(4):401–409.
36. del Rio A, et al. (2009) Stretching single talin rod molecules activates vinculin binding. *Science* 323(5914):638–641.
37. Grashoff C, et al. (2010) Measuring mechanical tension across vinculin reveals regulation of focal adhesion dynamics. *Nature* 466(7303):263–266.
38. Netti PA, Berk DA, Swartz MA, Grodzinsky AJ, Jain RK (2000) Role of extracellular matrix assembly in interstitial transport in solid tumors. *Cancer Res* 60(9):2497–2503.
39. Parker KK, et al. (2002) Directional control of lamellipodia extension by constraining cell shape and orienting cell tractional forces. *FASEB J* 16(10):1195–1204.
40. Lo C-M, Wang H-B, Dembo M, Wang Y-L (2000) Cell movement is guided by the rigidity of the substrate. *Biophys J* 79(1):144–152.
41. Vickerman V, Kamm RD (2012) Mechanism of a flow-gated angiogenesis switch: Early signaling events at cell-matrix and cell-cell junctions. *Integr Biol (Camb)* 4(8):863–874.
42. Montaño I, et al. (2010) Formation of human capillaries in vitro: The engineering of prevascularized matrices. *Tissue Eng Part A* 16(1):269–282.
43. Reinhart-King CA, Dembo M, Hammer DA (2008) Cell-cell mechanical communication through compliant substrates. *Biophys J* 95(12):6044–6051.
44. Deakin NO, Pignatelli J, Turner CE (2012) Diverse roles for the paxillin family of proteins in cancer. *Genes Cancer* 3(5-6):362–370.
45. Boucher Y, Jain RK (1992) Microvascular pressure is the principal driving force for interstitial hypertension in solid tumors: Implications for vascular collapse. *Cancer Res* 52(18):5110–5114.
46. Hofmann M, et al. (2006) Lowering of tumor interstitial fluid pressure reduces tumor cell proliferation in a xenograft tumor model. *Neoplasia* 8(2):89–95.
47. Shin Y, et al. (2012) Microfluidic assay for simultaneous culture of multiple cell types on surfaces or within hydrogels. *Nat Protoc* 7(7):1247–1259.
48. Zamir E, et al. (1999) Molecular diversity of cell-matrix adhesions. *J Cell Sci* 112(Pt 11):1655–1669.